PROTEINS: Structure, Function, and Genetics 53:307–319 (2003)

3D Structural Model of the G-Protein-Coupled Cannabinoid CB_2 Receptor

Xiang-Qun Xie,[1,2]* Jian-Zhong Chen[1] and Eric M. Billings[2]
[1]*Institute of Materials Science; and Department of Pharmaceutical Science, School of Pharmacy; University of Connecticut, Storrs, Connecticut*
[2]*Bioinformatics Core Facility, National Heart, Lung and Blood Institute, National Institutes of Health, Bethesda, Maryland*

ABSTRACT **The potential for therapeutic specificity in regulating diseases and for reduced side effects has made cannabinoid (CB) receptors one of the most important G-protein-coupled receptor (GPCR) targets for drug discovery. The cannabinoid (CB) receptor subtype CB2 is of particular interest due to its involvement in signal transduction in the immune system and its increased characterization by mutational and other studies. However, our understanding of their mode of action has been limited by the absence of an experimental receptor structure. In this study, we have developed a 3D model of the CB2 receptor based on the recent crystal structure of a related GPCR, bovine rhodopsin. The model was developed using multiple sequence alignment of homologous receptor sub-types in humans and mammals, and compared with other GPCRs. Alignments were analyzed with mutation scores, pairwise hydrophobicity profiles and Kyte-Doolittle plots. The 3D model of the transmembrane segment was generated by mapping the CB2 sequence onto the homologous residues of the rhodopsin structure. The extra- and intracellular loop regions of the CB2 were generated by searching for homologous C_α backbone sequences in published structures in the Brookhaven Protein Databank (PDB). Residue side chains were positioned through a combination of rotamer library searches, simulated annealing and minimization. Intermediate models of the 7TM helix bundles were analyzed in terms of helix tilt angles, hydrogen-bond networks, conserved residues and motifs, possible disulfide bonds. The amphipathic cytoplasmic helix domain was also correlated with biological and site-directed mutagenesis data. Finally, the model receptor-binding cavity was characterized using solvent-accessible surface approach. Proteins 2003;53:307–319.**

Key words: cannabinoid receptor subtype 2 (CB2); G-protein-coupled receptor (GPCR); 3D structure; homology; sequence alignment; computer modeling

INTRODUCTION

Cannabinoid (CB) receptor subtype CB2 was expressed in high quantities in human spleen and tonsils,[1,2] and was identified as a member of the rhodopsin-like family of seven-transmembrane (7TM) G-protein-coupled receptors (GPCRs). The CB2 receptor has been identified as a potential target for therapeutic immune intervention as its involvements in signal transduction processes in the immune system. Knowledge of the 3D structure of CB receptors will greatly aid in the rational design of specific CB2 ligands possessing potent therapeutic activities, but devoid from the undesirable side effects. However, its intrinsic membrane protein property makes it difficult to crystallize for X-ray study. Direct NMR studies are also restricted due to the large protein size and slow correlation time. So far, only one GPCR, bovine rhodopsin, has been obtained at high-resolution (2.8 Å) X-ray crystallographic structure.[3] Studies of the CB2 receptor to date have been limited by the lack of a three dimensional structure leaving many unanswered questions about the molecular level interactions between the receptor and its ligands as well as the nature of the receptor active site(s).[4]

Biochemical, pharmacological and computational investigations have provided insights into the cannabinoid receptors and their interaction with cannabimimetic ligands. Shire et al.[5] first demonstrated that the residues important for CB2 subtype specificity were located somewhere within the region of fourth transmembrane domain (TM4), extracellular loop 2 (e2) and fifth transmembrane domain (TM5) (TM4-e2-TM5). The same region was previ-

Abbreviations: GPCR, G-protein-coupled receptor; CB1, cannabinoid receptor subtype 1; CB2, cannabinoid receptor subtype 2; CNS, central nervous system; CD, circular dichroism; DMSO-d6, dimethyl-d_6 sulfoxide; DPC, dodecylphosphocholine; TM, transmembrane domain; BR, bacteriorhodopsin; e2, extracellular loop 2; CB2r_Human, human cannabinoid CB2 receptor of *Homo sapiens*; CB2r_mouse, mouse cannabinoid CB2 receptor of *Mus musculus*; CB1r_Felca, cat cannabinoid CB1 receptor of *Felis silvestris catus*; CB1r_Rat, rat cannabinoid CB1 receptor of *Rattus norvegicus*; CB1r _Human, human cannabinoid CB1 receptor of *Homo sapiens*; 5H2A_Rat, rat 5-hydroxytryptamine 2a receptor of *Rattus norvegicus*; DADR_Rat, rat D(1A) dopamine receptor of *Rattus norvegicus*; A2AA_Rat, rat alpha-2a adrenergic receptor of *Rattus norvegicus*; ACM1_Rat, rat muscarinic acetylcholine receptor m1 of *Rattus norvegicus*; SCR, structurally conserved regions; MM, molecular mechanic simulation; MD, molecular dynamic simulation; KD, Kyte-Doolittle method; NOE, nuclear Overhauser effect.

Grant sponsor: National Institutes of Health; Grant numbers: DA11510 and DA15770.

*Correspondence to: Xiang-Qun (Sean) Xie, U-3136, IMS, University of Connecticut, Storrs, CT 06269-3136. E-mail: xie@uconn.edu.

Received 31 October 2002; Accepted 12 May 2003

ously found to be important for binding of SR141716A to the CB1 receptor.[6] Furthermore, the ligand SR144528 was found to have a 700-fold higher affinity for the cannabinoid CB2 than the CB1 receptor.[7] It was recently discovered that Phe197 in helix TM5 region is crucial for the CB2 subtype specificity of another cannabinoid agonist, WIN55212-2.[8] It was proposed that the extracellular loop 2 (e2) dips down towards the binding pocket of SR144528 forming a sulfur-π interaction with the pyrazole group of SR144528.[8,9] A hydrophobic cluster of amino acids on helices TM6 and TM7 was identified as forming a hydrophobic binding pocket that increases ligand binding.[10]

Several computer models have been generated to explain the structure and biological function of CB receptors. Reggio et al.[11] constructed the first CB1 receptor model using the hydrophobic and variability moment vectors approach. Mahmoudian[12] later published a 3D model of the CB1 receptor based on the structure of bacteriorhodopsin (BR) and the helical alignments produced by the MULTALIGN program. Shire et al.[9,13] constructed CB1 and CB2 models on the basis of the rhodopsin data[14] reported by Baldwin. Computer-generated CB receptor models, site-mutagenesis studies, and biochemical/pharmacological data were discussed in their publication. Until the recent high-resolution X-ray structure of bovine rhodopsin became available, models of CB receptors and other GPCRs[15–17] had been based primarily on the structure of bacteriorhodopsin or low resolution X-ray data on the structure of rhodopsin. It had been widely assumed that the receptors had the same structure as bacteriorhodopsin, an integral membrane protein from *Halobacterium halobium*, whose seven-helical structure was known.[18] Nevertheless, the response of bacteriorhodopsin is not coupled to G proteins and its sequence shows none of the distinctive patterns of the receptor family. Consequently, models based on bacteriorhodopsin may not be representative of the GPCR superfamily.[19] This warranted a new effort to develop a model based on the experimental rhodopsin structure as a representative of the GPCRs for an improved understanding of CB2 structure.

In this study, we developed and refined a 3D model of the CB2 receptor by using established multiple sequence alignment methods[20] and the recently-published, high-resolution X-ray structure of bovine rhodopsin.[3] The validity and applicability of the model is then examined. It is known that members of the GPCR superfamily share considerable structural homology, reflecting their common mechanism of biological action. More than 100 members of this large family of receptor proteins have been sequenced, and they are characterized by seven hydrophobic stretches of about 26 amino acid residues that are predicted to form transmembrane α helices. The helices are connected by alternating extracellular and intracellular loops. Homology modeling benefits from these specific motifs since it has been established that amino acid sequences and structures are highly conserved in biologically important regions.[21]

The initial models were constructed and then optimized using molecular simulation methods including rotamer library searches for amino acid side chains, molecular dynamics and energy minimization. Intermediate CB2 models were then critiqued by analyzing the hydrophobicity of helical segments, helix tilt angles, and relative positions of the helices. The inter-helix hydrogen bond interactions were also mapped out. Furthermore, the potential disulfide bonds, the local structure due to common GPCR sequences and the cytoplasmic helical segments as well as the possible ligand-binding cavity, were considered in the 3D model. The calculated CB2 models were subjected to refinement under the constraints determined by using multidimensional isotope-editing NMR experiments, which are currently under way, and the results will be described elsewhere. The CB2 model is expected to provide working hypotheses that are useful for subsequent biochemical studies and as a basis for rational drug design methodologies.

METHODS

Multiple Sequence Alignment

The sequence alignment of the target CB2 receptor was based on the observation that the GPCR family is characterized by seven hydrophobic stretches, predicted to form transmembrane α helices, connected by alternating extracellular and intracellular loops.[22] It is also known that the primary sequence of GPCRs possesses high sequence homology in hydrophobic transmembrane domains, whereas the hydrophilic loop regions are more divergent. In general, there are three challenging aspects regarding the construction of an initial homology-based model that should be considered. These include sequence alignment, loop structure formation and establishing side-chain conformations.[23] To perform accurate multiple sequence alignment, we have chosen ten complete GPCR sequences from the GPCR database.[24] These ten GPCR sequences were selected since they are classified in the same rhodopsin-like super family of the GPCRs and contain the most highly conserved residues[11,14] in their seven transmembrane spanning domains. These GPCRs include the human cannabinoid CB2 receptor of *Homo sapiens* (CB2r_Human),[1] mouse cannabinoid CB2 receptor of *Mus musculus* (CB2r_mouse),[25] cat cannabinoid CB1 receptor of *Felis silvestris catus* (CB1r_Felca),[26] rat cannabinoid CB1 receptor of *Rattus norvegicus* (CB1r_Rat),[27] human cannabinoid CB1 receptor of *Homo sapiens* (CB1r _Human),[28] rat 5-hydroxytryptamine 2a receptor of *Rattus norvegicus* (5H2A_Rat),[29] rat D(1A) dopamine receptor of *Rattus norvegicus* (DADR_Rat),[30] rat alpha-2a adrenergic receptor of *Rattus norvegicus* (A2AA_Rat),[31] rat muscarinic acetylcholine receptor m1 of *Rattus norvegicus* (ACM1_Rat),[32] and bovine rhodopsin.[3]

First, we aligned the CB2 sequence with the target GPCRs using a series of pairwise and multiple sequence alignments. The initial sequence alignment of the CB2 receptor was carried out using automatic sequence alignment of CB2 with four cannabinoid receptors (CB2r_Mouse, CB1r_Felca, CB1r_Rat, and CB1r_Human) using the PAM 120 Mult Scoring Matrix and default values in the InsightII/homology module.[20] Then, manual multiple sequence align-

ments were conducted to locate the homology aligned regions using MSI Biosym software for all 10 GPCR sequences described above. Once the CB2 receptor is initially aligned, the regions over which the sequences are mutually related can be located and the statistical significance of their relationship estimated. Those regions containing highly significant relationships are likely to contain structurally conserved regions (SCRs). Calculations were based on the segment pair overlap algorithm[33] to identify the blocks of mutually related sequence segments. The algorithm is also a true multiple alignment algorithm in the sense that all sequences are compared simultaneously, and the results are independent of the ordering of the sequences.[20] The algorithm imposes no arbitrary limits on the possible length of the target block. Then, the similarities of the sequences were calculated using the PAM 120 Mult Scoring Matrix,[34] which is more selective and tends to find m-blocks that are more likely to be structurally conserved than the PAM 250 Mult Scoring Matrix.[20] The description of the Mult Scoring Matrix techniques was detailed in Dayhoff's publication.[34] Gaps were manually inserted into the sequences to bring the contents of the blocks into alignment.

The aligned sequences were then evaluated with the hydrophobicity scoring matrix[20] to assess the transmembrane, intra- and extracellular segments of the CB2 receptor and the other nine receptor sequences. The average value of all ten calculated hydrophobic scores of corresponding segments was computed to determine the corresponding regions of high hydrophobicity. The segments that satisfy the two requirements: i) high mean score of multiple sequence alignment and high average hydrophobic score; and ii) the middle ~18 residues of each helix are approximately perpendicular to the membrane and their polar residues (not facing out into the lipid) are predicted to be in the transmembrane domain of protein. For example, the block, which contains the residues from Pro31 to Ile59 for CB2r_human sequence (Fig. 1), has slightly a lower mutation score and hydrophobic score, but its polar and non-polar side chains have proper positioning as described above. Therefore, it was identified as the helix I segment. The other six helical segments were determined using a similar approach. The completed multiple sequence alignment for the ten GPCRs sequences is shown in Figure 1. Noticeably, helix V in the cannabinoid receptors lacks the highly conserved proline residue of the other rhodopsin-like GPCRs, whereas the second highly conserved residue Tyr in Helix V[11,14] of the ten GPCRs was identified and aligned unambiguously. The present alignment for Helix V was also congruent with the reported CB1 receptor studies by Reggio et al.[11]

Hydrophobicity Profile Analysis

The identified transmembrane segments were further examined for the consistency of the relative hydrophobicity values of homologous amino acids in the protein sequence. Since the hydrophilic residues for GPCRs tend to be buried in the interior of the molecule and the hydrophobic residues are more exposed to cellular membrane, a profile of these values can indicate the overall folding pattern. In this study, we applied the Kyte-Doolittle (KD) method to perform the hydrophobicity analysis of the identified transmembrane regions by visualizing the hydrophobicity of a protein along its sequence. Since proteins do not fold based on the tendencies of single residues, but rather on the characteristics of larger groups of residues, a running average of the hydrophobicity values of the residues is more appropriate. The moving window averaging technique was applied to identify regional effects using a window of seven.[20,35] The hydrophobicity scale is divided into three hydrophobicity levels: hydrophobic (0.7), neutral, and hydrophilic (−2.4), as defined in the Kyte-Doolittle scale.[36] The averaged hydrophobicity profiles are shown in Figure 2 and are consistent with the predicted seven transmembrane domains.

Model Assembly

Due to the lack of sufficient structural constraints, the first 25 residues (residues 1-25) in the N-terminus and the last 41 residues (residues 320–360) in the C-terminus were excluded from the model. In addition, we knew from the literature that the N-terminus of the cannabinoid receptor family contributes little to the ligand binding affinity and the C-terminus is located on the intracellular side. Such an omission should not significantly affect the prediction of the seven helical bundles GPCR model as discussed below.

Construction of the helices of CB2 receptor

The CB2 helical domains were constructed based on the assumption that all members of the GPCR family have the same basic structure in the membrane-embedded part of the protein. The transmembrane segments are believed to be α helices and oriented roughly perpendicular to the membrane as in rhodopsin.[3] We therefore used the 3D X-ray crystallographic structure of bovine rhodopsin registered in PDB as a direct template to construct the 7 TMs helical structure of CB2 using the InsightII homology module.[20]

Searches of the variable/loop regions

Putative structures of the loop regions were determined by a database search of all protein Cα distances in the PDB bank. The beginning four and the ending five residues of each loop segment were generated using the InsightII Homology "endpair" facility.[20] The backbone conformations of loop regions were generated for the nine residues on the N- and C-terminals were then extended. The ten most preferred conformations obtained for every loop region were inspected visually for their steric interactions with the local environment. The loop conformation with the fewest steric clashes, reasonable packing and the smallest R.M.S. deviation at the terminal residues was selected. Then, InsightII Homology "SpliceRepair" facility[20] was used to adjust backbone bond distances for the connection of the helix and loop region, removing the irregular C-N distances and torsion angles of the terminal residues generated in the loop search process.

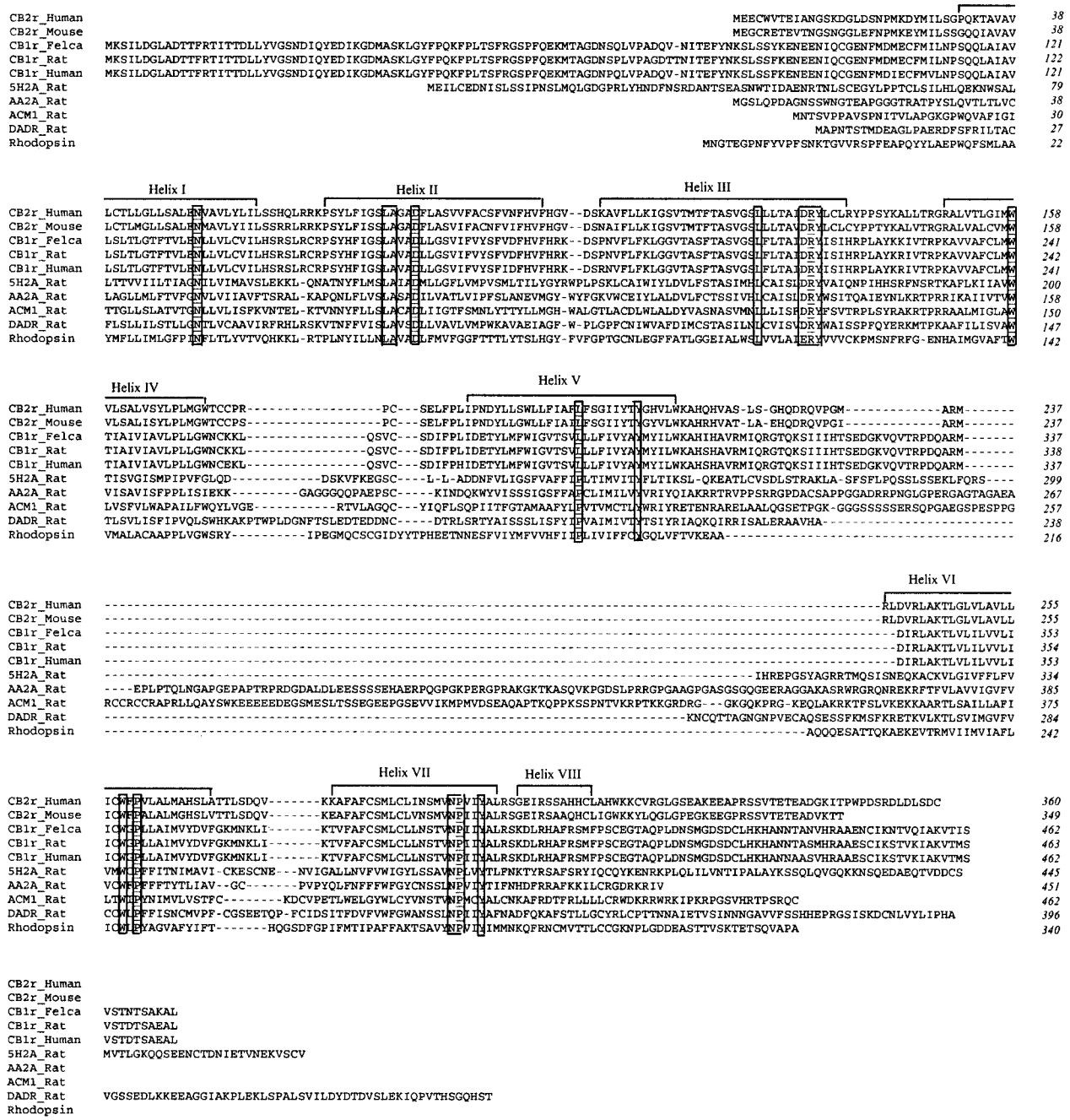

Fig. 1. Multiple sequence alignment and homology study of ten GPCR sequences. The highly conserved residues and GPCR motifs are highlighted in boxes.

Generation of the side-chain conformation

The prediction of side-chain conformations is a challenging task due to the combinatorial explosion of possible side-chain placement. Fortunately, statistical studies of protein structures show that side chains usually adopt only a small number of the many possible conformations available to them. Typically, an amino acid side chain can be specified with 2χ angles representing four to six commonly seen conformations or rotamers.[37] All of these common conformations are combinations of the familiar gauche and anti moieties. For longer side chains, more combinations of the allowed χ angles make for a greater number of possibilities. In our calculation, the InsightII Homology "Residue/Auto-_Rotamer" module[20] was used to sample the rotamer library for each of the 20 amino acid types for identifying the rotamer with optimum steric interactions.

Structure Optimization

Many structural artifacts were introduced into the receptor model as it was being built. These include the

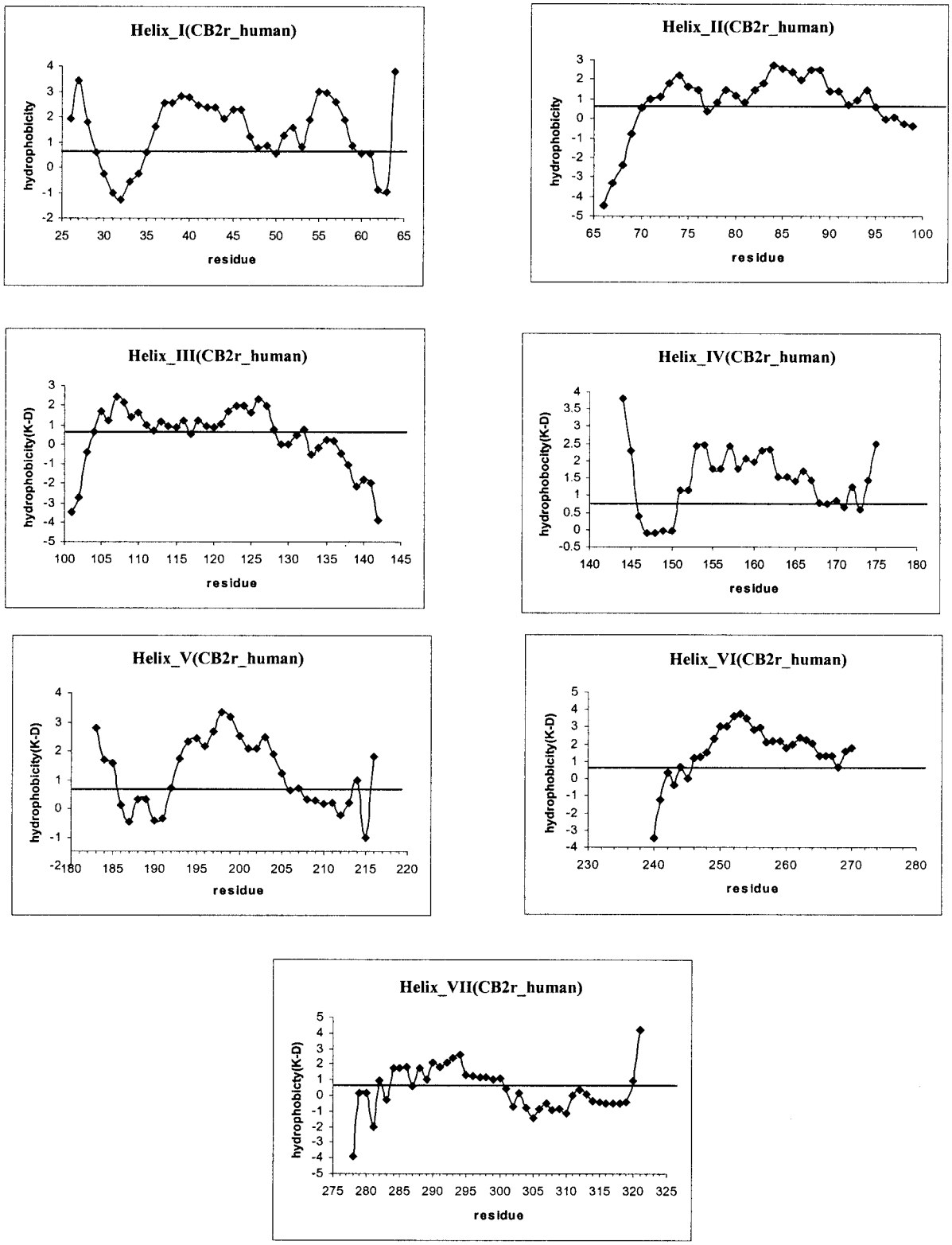

Fig. 2. Kyte-Doolittle hydrophobicity plots, showing three hydrophobicity levels: hydrophobic (0.7), neutral, and hydrophilic (−2.4).

substitution of large side chains for small ones, strained peptide bonds between segments taken from different reference proteins, and sub-optimal loop conformations. All of these artifacts can be reasonably addressed with further optimization using energy minimization and molecular dynamics (MM/MD). In our study, we applied the

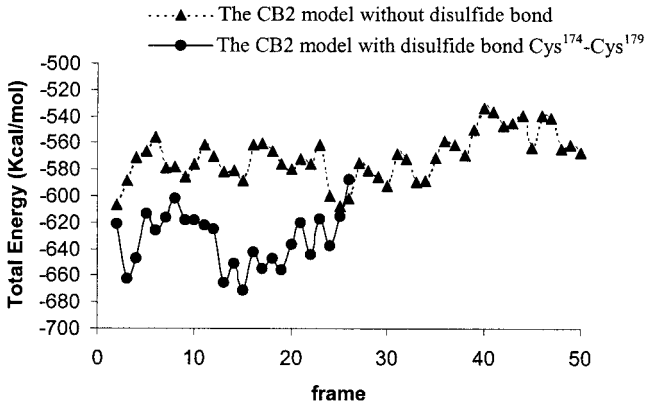

Fig. 3. Total energy of the trajectory of CB2 during the molecular dynamics simulation. Several snapshots were retrieved for further structural optimization by energy minimization.

AMBER force field with a 15 Å cut-off distance for non-bonded interactions to optimize the intermediate CB2 receptor model. In order to mimic the different biological environments for transmembrane and loop domains in the calculations, we set the dielectric constant to a value of 5 for the hydrophobic transmembrane environment and the dielectric constant 80 for the hydrophilic loop environment in the two phases of computer simulations. The molecular dynamics protocol consists of: i) initial minimization for 500 iterations of steepest descents, followed by conjugate gradients minimization, until the root-mean-square deviation (RMSD) became less than 0.1 kcal $mol^{-1}Å^{-1}$. ii) MD simulations were then performed at a constant temperature of 1000 K and a time step of 1 fs. Initially, a constraint was applied to keep the backbone atoms in the seven TM domains. Fifty representative snapshots from the molecular dynamics run were retrieved, minimized with 500 iterations of steepest descent, and followed by conjugate gradient minimization until the maximum derivative was less than 0.1 kcal $mol^{-1}Å^{-1}$ without any constraints.

Predicting Potential S-S Bond Formation

Representative snapshots of the CB2 model from the molecular dynamics indicated that Cys174 and Cys179 are in close proximity and may form a disulfide bond. This was supported by further MD/MM on the CB2 structure with disulfide bonds in place. The MD simulations were performed using the protocol described above with a disulfide bond between Cys174 and Cys179. Twenty-five representative snapshots recorded during the dynamics run were retrieved and minimized using steepest descent and then conjugate gradient minimization until the maximum derivative was less than 0.1 kcal $mol^{-1}Å^{-1}$. Analysis of the two MD simulations suggested that the CB2 conformer model with the disulfide bond has the lower energy. The detailed results and discussion are provided later. Figure 3, which shows the energy of the trajectories in both MD simulations, indicates that the model with two disulfide bridges has the lower energy conformation.

Identifying Cytoplasmic Helix Domain (or Helix VIII)

Analysis of the CB2 model on the basis of homologous residues in rhodopsin showed the existence of an additional cytoplasmic helix domain. To confirm this, we have synthesized a peptide representing Ile298-Lys319, which encompasses the sequence of the helix 8 region of the CB2 receptor. The secondary structure of this peptide was determined by NMR and CD under different solvent environments, including water, DMSO, and DPC micelles. Circular dichroism (CD) spectra were recorded on a Jasco J-715 spectrometer. Spectra were recorded as mean reside molar ellipticity. Quantification of the secondary components was done by comparison with computed spectra of model systems.[38] NMR spectroscopy—sample of peptide in DMSO-d6, D_2O and DPC micelles contained 2.4 mM of peptide (H_2O/D_2O, 90%/10%, v/v) at pH5.5. The 2D NMR NOESY spectra were recorded with a mixing time of 300 ms for the water and DMSO, and 150 ms was eventually selected for the NOE assignments of the DPC micelles sample. The detailed experiments are presented elsewhere.[39]

Mapping the Inter-Helix H-bond Network

We have developed scripts that allow us to automatically search for the inter-helix hydrogen bonds under two defined criteria: the H-bond distance is less than 3.0 Å and the donor-proton-acceptor angle is in the range of 120°~180°. The inter-helix H-bond information is used to evaluate the 7TM structure of the CB2 model as described later.

Probing the Intramolecular Channel Cavity by Using MOLCAD

The channel cavity of the CB2 model was compared with observed characteristics of other transmembrane receptors. Several properties, such as electrostatic potential, hydrophobicity, hydrophilicity and lipophilicity were mapped onto a MOLCAD-generated molecular surface. The solvent-accessible (Connolly) surface was generated using the MOLCAD program (SYBYL, version 6.8).[40] MOLCAD's rendering techniques allow the rapid calculation and display of the property-coded surface for the molecular recognition.

RESULTS AND DISCUSSION

A graphical representation of the two-dimensional CB2 model is shown in Figure 4. It reveals that the 294 amino acids of CB2 with truncated amino acids on N- and C-terminals, 25 and 41 residues respectively, fold into seven transmembrane helices, extra- and intra-cellular loops, as well as a cytoplasmic helix (or helix VIII). Similar to bovine rhodopsin, the human cannabinoid receptor CB2 is classified as a member of the largest subgroup I of GPCRs, class A rhodopsin-like,[24] with its helices being tilt at various angles with respect to the membrane surface. Both are also expected to contain a mix of α- and 3_{10}-helices and possess a certain number of kinks, twists and bends.[41,42]

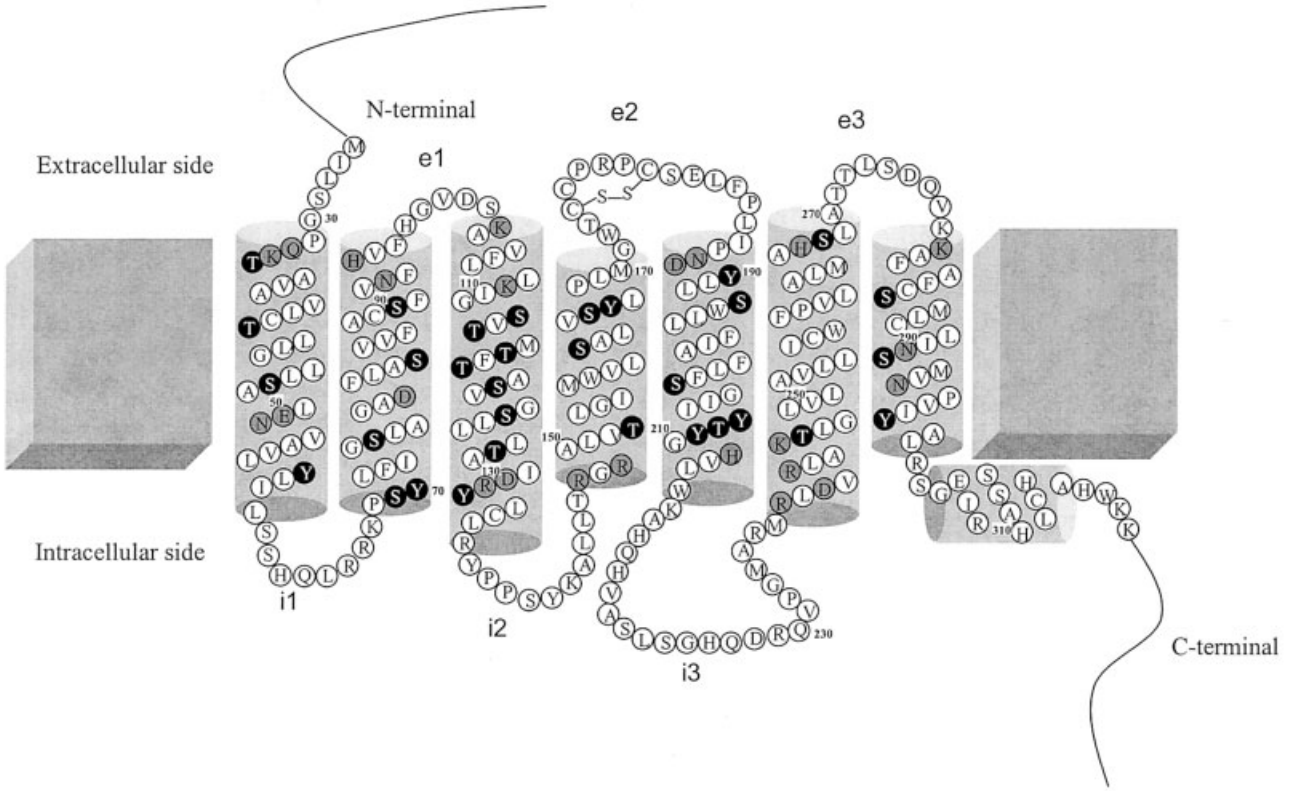

Fig. 4. Two-dimensional model of cannabinoid receptor CB2. In the transmembrane domains, shadow circles represent the hydrophilic residues, and the black circles represent the residues with an OH group. These side chains would not be directed into the hydrophobic region of the membrane. Our model suggests that a disulfide bond may be formed between two cysteine residues in the e2 region.

Helix Tilt Angles

To determine the helix tilt angles, the helix VIII domain (detailed later) was assumed to lie relatively parallel to the membrane with a tilt angle of 90°.[42] The helix tilt angles are defined as the angles between the helical axes and the long axis of the GPCR molecule or membrane plane.

Our results show that helix I is tilted from the plane of the membrane by 22°, and helix II is off 24° (Fig. 5). Helix III is the longest TM segment, extending from the residue Lys103 to Arg136 (Fig. 4) and it has the largest tilt angle, 26° from the plane of the membrane (Fig. 5). This results in helix III being in close contact with the rest of the helices except helix I through inter-helix hydrogen bonding and other non-bonded intermolecular interactions that are discussed later. Helix IV is the shortest TM segment consisting of 25 residues, and runs almost perpendicular to the membrane with a 5° tilt angle. Helix V has a length of 29 residues and is tilted 7° from the membrane normal. A "kink" (bent angle ~32°) was observed on helix VI domain of the CB2 model, and is attributed to the presence of the residue Pro260, one of the most conserved residues among GPCRs. Helix VI was measured showing two tilt angles, 32° and 10°, correspondent to the extra- and intra- cellular helical segments with respect to the membrane plane. Helix VII's tilt angle is measured as 25° from the membrane plane. Figure 5 provides a graphic view of the CB2 seven transmembrane helix bundles displaying the helix relative positions and helix tilt angles.

Inter-Helix Hydrogen-Bonding Network

An analysis of inter-helix hydrogen bond and non-bonded interactions shows that in addition to hydrophobic interactions, there is an extensive inter-helix hydrogen-bond network formed among these helices. This contributes to the stabilization of the seven transmembrane domains of CB2 receptor structure. As shown in Figure 6, helix III positions itself in close contact with the rest of the helices except helix I through inter-helix hydrogen bonding (e.g., Phe87-Ser112, Leu126-Arg149, Leu125-Thr208, Phe117-Trp258, Ser120-Asn295) and other non-bonded inter-helix interactions, such as the hydrophobic interaction between non-polar side chains (e.g., Ala83-Met115, Leu76-Ala119, Ile110-Pro168, Leu133-Leu145, Val121-Leu201, Leu125-Ile205, Leu124-Leu251, Leu124-Leu254, Val113-Leu289). Another example is that helix IV has inter-helix hydrogen bonds (e.g., Ser75-Trp158, Asn188-Leu167, Ser165-Ala111) and hydrophobic interactions (e.g., Leu154-Leu71, Ala150-Leu75, Leu167-Leu192, Val164-Phe197, Leu160-Phe197, Leu145-Leu133, Pro168-Ile100, Leu169-Leu101) with helices II, III, and V. Other hydrogen bond interactions were also detected among helix I with adjacent helix II and helix VII. Its inter-helix interactions are also strengthened by hydrophobic interactions among Leu43, Phe87, Phe91, and Leu289; helix II with helices I, III, IV, and VII; and helix V with helices III and IV. Helix VI only has inter-helix hydrogen bond interactions with helix III, whereas it interacts with helices II, V,

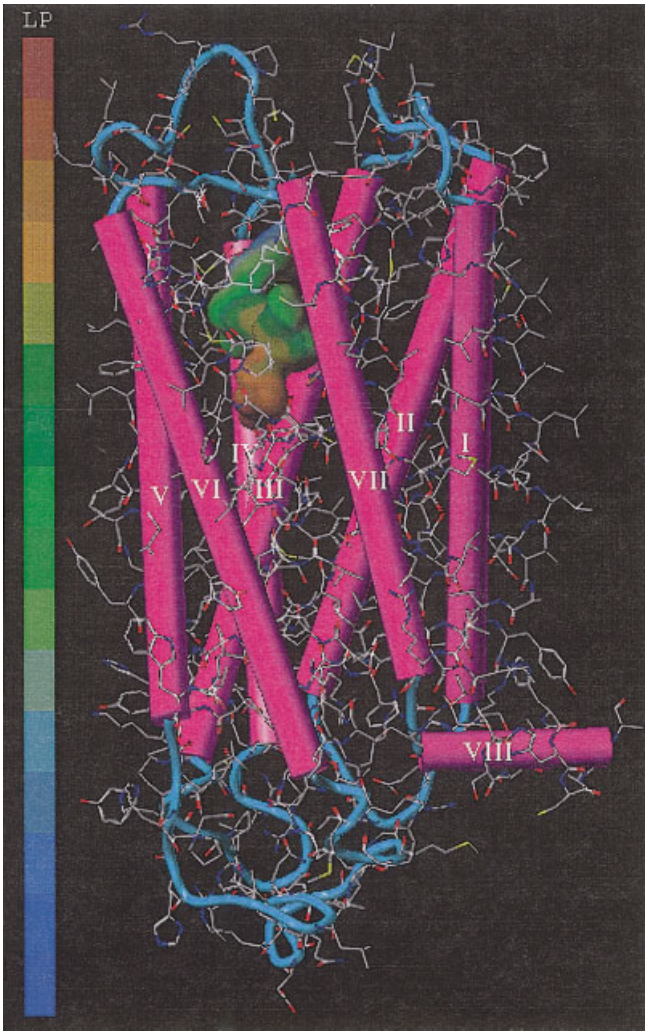

Fig. 5. Three-dimensional model of the CB2 receptor. Helical portions of the protein, including the seven transmembrane helices, are shown as violet cylinders. Loop regions are shown as blue ribbons. A solvent-accessible surface representing the model's receptor binding cavity shows an amphipathic region near the transmembrane helices III, V and VI. A lipophilicity scale is displayed.

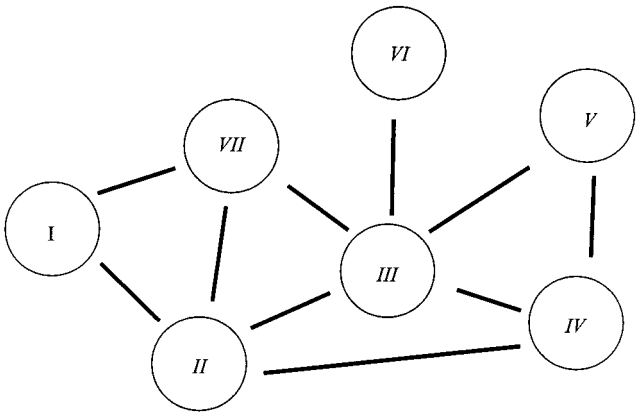

Fig. 6. An extensive inter-helix hydrogen-bonding network is present in the model. The seven transmembrane helices are stabilized by these and van der Waals interactions.

and VII through van der Waals interactions. It is hypothesized that such weak interactions give certain elasticity to helix VI with respect to the rest of the helices. Such a relative mobility of the helix VI may be involved with GPCR receptor activation.[42–44] There is no hydrogen bonding but rather van der Waals interaction between the helix VII and VI, whereas the helix VII does show hydrogen bond interactions with the rest of the helices except helices IV and V.

Conserved Residues and Motifs

Cannabinoid receptors are integral membrane proteins whose amino acid sequences are characterized by seven hydrophobic segments containing distinctive patterns. The calculated CB2 model shows that the residues in each helical segment can be classified into two groups consistent with other reported GPCRs:[19] i) Residues facing toward membrane lipids are typically hydrophobic ones, including non-polar residues Phe, Met, Trp, Ile, Val, Leu, Ala, and Pro, and three uncharged polar residues Ser, Thr and Tyr; ii) Residues facing towards the central core of the helix bundles and not expecting to be in contact with lipid are polar or charged residues including Asp, Glu, Cys, Asn, Gln, Thr, Tyr, Ser, Gly, His, Lys, and Arg. Figure 7 shows that Asn51, a highly conserved residue in the GPCR family, is located in the intracellular side of the helix I, and faces towards the center core of the CB2 receptor as it is a hydrophilic polar residue. The LAXXD motif (Fig. 1) of GPCRs is also observed in the CB2 helix II domain with their side chains of the highly conserved Leu76 and Asp80 pointing toward the 7TM core. In addition, the side chain of the polar residues Asp80, Ser112, Thr116, Ser120, Gln291, and Gln295 are grouped together whereas the residues Ser112-Thr116-Ser120-Gln295-Gln291 except Asp80 tend to form a cluster through H-bonding network that secures helix bundles. The observation confirms the CB2 Asp80 mutation data that Asp80 did not play key roles in CB2 receptor binding or structural conformation.[10] CB2 Ser112 is near the predicted hydrophilic center, and has been shown to be crucial for the recognition of several cannabinoid ligands in CB2 receptor binding based on the mutagenesis studies of S112G.[45] The homologous residue in the CB1 TM3 domain is Gly195 as shown in the alignment studies (Fig. 1). Unlike the CB1 receptor in which residue Lys192 plays an important role for the binding of most of cannabinoid ligands,[46] the homologous conserved residue Lys109 in the CB2 TM3 domain does not appear to be a key residue.[45] The dissimilarity between CB2 Ser112 and CB1 Gly195 as shown in the multiple sequence alignment may account for the ligand binding discrepancy between CB2 and CB1 molecules. Such a subtle difference between two receptors could be exploited to design CB2 specific ligands in the future.

CB2 helix III is in contact with the other helices and plays important roles in the regulation of cannabinoid receptor activities.[45] It was also noticed in our calculated CB2 model that helix III contains highly conserved residue

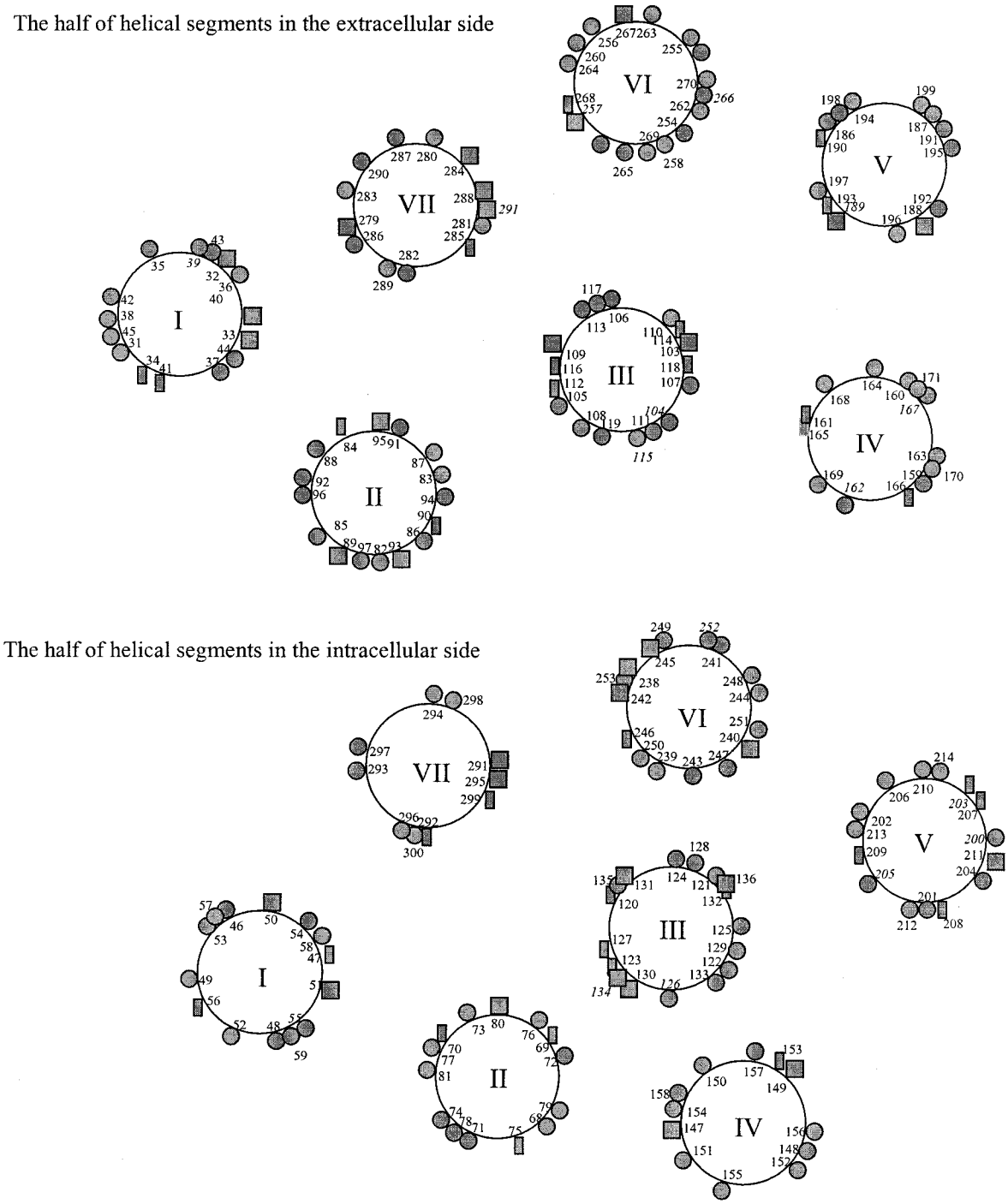

Fig. 7. Helical wheel plots are shown for the seven transmembrane segments. The α-carbon positions are shown in the inner ring: black circles (●) indicate hydrophobic residues; black square (■) indicate hydrophilic residues and black rectangular (▮) indicate the residues with a hydroxyl group.

Leu124 facing towards the 7TM core, and an important GPCR motif D(E)RY situated near the cytoplasmic side of helix III (Fig. 1 and Fig. 5). The D(E)RY motif exists in most GPCRs and was implicated in the regulation of the receptor's interaction with its G-protein.[42] Similar to bovine rhodopsin,[42] the residues Asp130 and Arg131 in CB2's DRY motif are observed in a hydrophobic environment formed among residues (Pro68, Leu133, Leu135, Leu145, Leu243, Ala244). However, our results also revealed that the CB2 Arg131 has a charged interaction with residue Asp260 in the cytoplasmic end of the TM6, forming a salt bridge (data not shown). This is consistent with the high-resolution X-ray crystal structure of bovine rhodopsin.[42] It has been reported in mutation studies on beta-2-adrenergic[47,48] and serotonin 5-HT2a[49] that this key salt bridge would serve to constrain the rhodopsin-like recep-

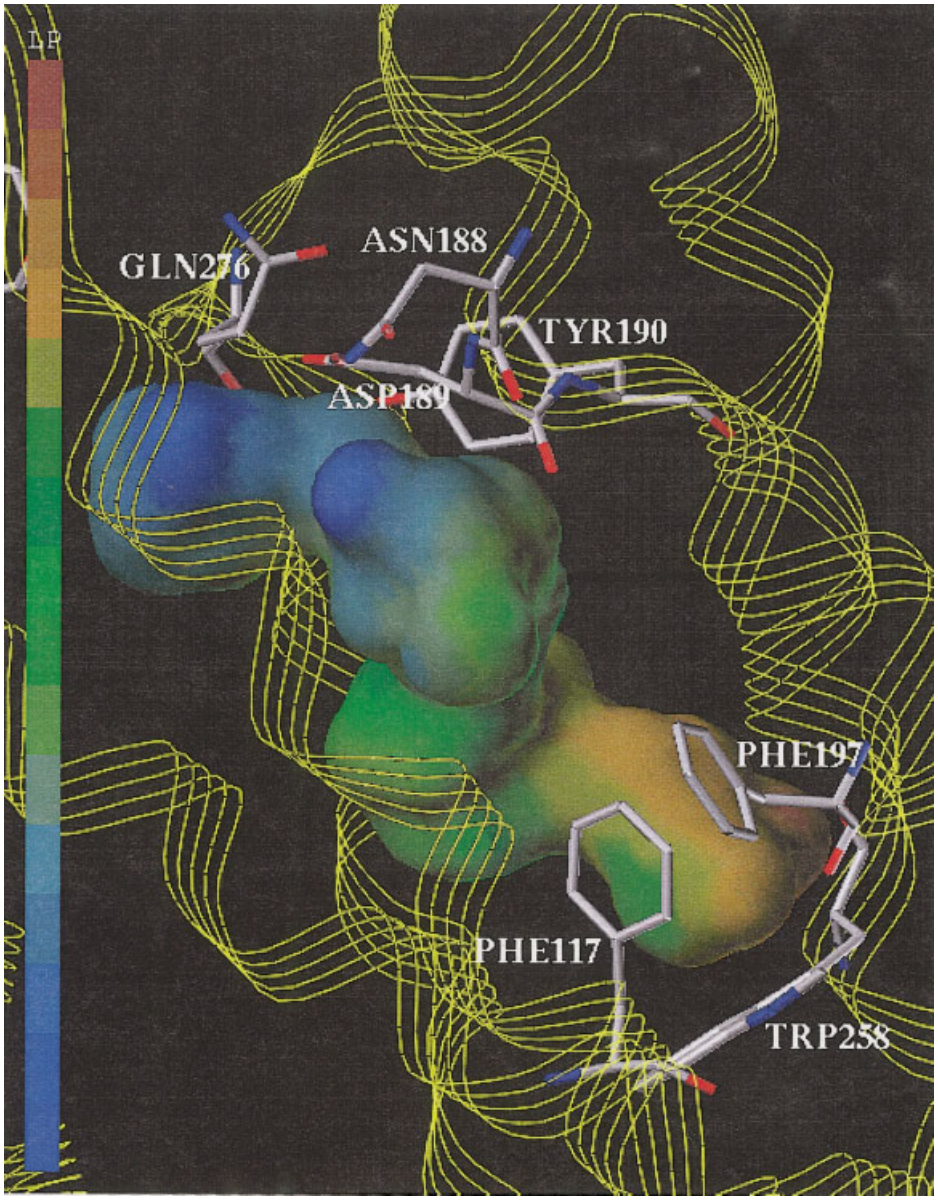

Fig. 8. The amphipathic cavity of the CB2 model is approximately bounded by the solvent accessible surface shown. A putative binding site for CB2 ligands is located adjacent to helices III, V, and VI. The surface is colored using the lipophilicity scale in which the hydrophilic center (blue) is framed by polar residues. A hydrophobic cleft (brown) is surrounded by aromatic residues.

tor in the inactive state and breaking the salt bridge could be a key step in receptor activation.[43] It is hypothesized that the cannabinoid receptor might assume a similar activation mechanism.

Mutagenesis studies indicate that the TM4 domain in the CB2 receptor plays more important roles for the recognition of the cannabinoid ligand than in the CB1 receptor. The CB2-selective antagonist, SR144528 completely failed to antagonize the CB2 mutant of S161A or S165A,[9] which is readily explained by our multiple sequence alignment showing that the homologous two sites in the TM4 domain of the CB1 receptor are occupied by the residue Ala (Fig. 1). The study confirmed that these two serine residues are likely to be involved in binding of the CB2-preferred antagonist SR144528.

In contrast to earlier computer models[8,9,50] prior to the crystal structure of the bovine rhodopsin,[3] our model does not display the significant hydrophobic region formed by aromatic residues Trp172, Trp194, and Phe197. Instead, our solvent-accessible surface calculation revealed a new potential binding domain as depicted in Figure 8, showing amphipathic molecular surfaces located in a cavity among the helix III, V, VI, and VII on the extra-cellular side of the 7TM bundles. As shown, with the lipophilic scale being displayed in Fig. 8 (left side), the surface cavity consists of a hydrophilic center pointed towards the e2 loop interface

and framed by the polar residues Asn188, Asp189, Tyr190, and Gln276, and a large hydrophobic cleft (brown) surrounded by hydrophobic aromatic residues Phe117, Phe197, and Trp258 of the transmembrane domains III, V, and VI. The distance between the hydrophilic and hydrophobic centers is estimated as 9–11 Å, which is about the size of WIN55212-2 molecule. The residues S161A or S165A are located in proximity (~ 4–6 Å) of the cavity, and are about 8 Å to the predicated hydrophobic cleft. The model is consistent with the CB2 mutant of F197V that resulted in a 14-fold decrease of WIN55212-2 binding affinity[8] whereas CP55940 and anandamide binding were least affected.[8,50] The model also indicated that there are more than one plausible binding site and orientation for CB ligands. Further verification of the predicted binding model will require additional site-directed mutagenesis studies. Additional receptor docking calculations are currently under way.

In addition, the CB2 model reveals that residue Tyr299 (helix VII) near the intracellular loop participates in inter-helix H-bonding with Ser303 (loop i4), and Ser69, Tyr70 (helix II). Such hydrophilic interactions among these residues stabilizes the helices II, VII, and VIII interaction, and is consistent with the recent mutagenesis study[51] showing that Tyr299 is a crucial residue for the receptor's conformation. This observation is also concordant with the rhodopsin discussion by Teller[42] in which the motif NPXXY in the helix VII is considered highly conserved among GPCRs, and is predicted to be involved in the formation of a structural domain that would allow it to interact with helix VI by holding rhodopsin in the inactive state. In contrast, we did not detect the hydrogen bonding interactions between helix VII and VI in the CB2 model, but rather extensive van der Waals non-bonded interactions. Other conserved GPCR residues are highlighted in Figure 1.

Disulfide Bond Bridge

It is known that conserved cysteine residues in GPCRs may form an intramolecular disulfide bridge (S-S) that links extracellular loops of the receptors. The disulfide bond constrains the conformation of the extracellular domains of the protein and stabilizes the transmembrane structures.[52–54] Lu et al. have reported that the integrity of the disulfide bridge is important for [^{3}H] CP-55,940 binding to the cannabinoid receptor.[55] Our unconstrained CB2 model predicted that there is a possible disulfide bond bridge formed in the extracellular loop e2 region since the two residues Cys174 and Cys179 are in close proximity during the molecular dynamics simulation. This was examined by a second molecular dynamics simulation and energy minimization with an S-S bond between Cys174 and Cys179 (2 Å). The disulfide bond is readily incorporated in the model and the total conformational energy is reduced. This result is consistent with the site-mutagenesis studies reported by Gouldson et al.[9] In their studies, the conserved cysteine residues in the loop e2 of CB2 receptor were independently mutated to serine, which resulted in correctly translocated receptors as evidenced by immunofluorescence measurements which, however, failed to bind any of the cannabinoid ligands tested. Clearly, these cysteine residues assume an important structural role in cannabinoid receptors rather than being involved in ligand interactions. Further biochemical and biophysical experiments would be required to provide additional information to understand the roles of disulfide bonds in the receptor structures and bioactivities.

Amphipathic Cytoplasmic Helix

In addition to the 7TM helices described above, there is another short helix domain from Gly304 to Leu314 in the cytoplasmic surface of the CB2 receptor. This was identified in our computational work and has been confirmed by our NMR experimental studies of the synthetic peptides Ile298-Lys319 in a membrane-like environment reported elsewhere.[39] This is also consistent with the X-ray crystallographic structure of bovine rhodopsin.[3] Our data showed that the hydrophobic residues on helix VIII are located on one side of the helix with a separation of roughly one helical turn apart, whereas the cationic hydrophilic side chains, such as histidine, arginine and lysine, are situated on the other side, making the structure amphipathic as a whole.

The amphipathic characteristic of helix VIII reveals some interesting structural and functional aspects. It was found in other similar studies[56] that when a cationic, amphipathic α-helical peptide such as helix VIII is bound to a phospholipid bilayer, it maintains a position parallel to the plane of the membrane with its hydrophobic face within the bilayer and its positive charges (in this case the Arg307, and His311, as well as extended residues Lys318) facing toward the cytoplasmic medium.[57,58]

It should be pointed out that this amphipathic helix VIII structure is also observed in other GPCRs family, such as rhodopsin,[3] and the β-adrenergic receptor.[59] In particular, emerging studies indicate that this region is responsible for the G-protein binding and activation.[56,60–63] The same region has also been suggested to have binding interaction with the Gtα subunit of the G-protein.[60] The implication of this feature being shared by numerous GPCRs can be significant.[57,64] The detailed NMR experimental and discussion of the helix VIII fragments is published elsewhere.[39] Further investigation of helix VIII by other means, such as mutagenesis or protein binding studies, may yield additional information regarding the structural and functional aspects of this potentially important region.

SUMMARY

We have constructed a theoretical, three-dimensional model of the human cannabinoid receptor subtype CB2, and predicted the associated structural information including helix structures, inter-helix hydrophobic interactions, inter-helix H-bond networks and a possible disulfide bond as well as the predicted possible binding surface within the 7TM bundles. The CB2 transmembrane domains were determined by homology multiple sequence analysis methods and the loop regions were defined by a thorough search of the protein backbones in PDB bank. Subsequently, a 3D

structure of CB2 receptor was generated on the basis of the template of the recently published X-ray crystallographic structure of bovine rhodopsin. Finally the model was refined through molecular dynamics simulations and energy minimization. The model was shown to correlate well with known biochemical results, site-directed mutagenesis studies and known X-Ray crystallographic and NMR studies. The 3D model's integrity was examined by systematic comparisons of hydrophobicity profiles, analyses of helix tilt and packing properties, search of inter-helix hydrogen bonding interactions, and investigation of the conserved residue positions and motif compositions. In addition, a cytoplasmic helix was identified in the CB2 receptor by both computer modeling and NMR experiments. In contrast to earlier studies, novel putative binding sites and their basis have been identified. Further studies are under way to obtain additional structural data about the CB2 receptor by using isotope-editing multidimensional high-resolution NMR techniques that will be reported elsewhere.

ACKNOWLEDGMENTS

We thank Dr. P.H. Reggio for her professional discussions. We thank Dr. A. Makriyannis for his collaboration on this project. We also acknowledge Drs. M. Miller, F. DiCapua, and Pfizer Inc. for providing support with the computer molecular modeling packages.

REFERENCES

1. Munro S, Thomas KL, Abu-Shaar M. Molecular characterization of a peripheral receptor for cannabinoids. Nature (London). 1993; 365:61–65.
2. Galiegue S, Mary S, Marchand J, Dussossoy D, Carriere D, Carayon P, Bouaboula M, Shire D, Le Fur G, and Casellas P. Expression of central and peripheral cannabinoid receptors in human immune tissues and leukocyte subpopulations. Eur J Biochem 1995;232:54–61.
3. Palczewski K, Kumasaka T, Hori T, et al. Crystal structure of rhodopsin: A G protein-coupled receptor. Science 2000; 289:739–745.
4. Berlose JP, Convert O, Brunissen A, Chassaing G, Lavielle S. Three dimensional structure of the highly conserved seventh trans membrane domain of G-protein coupled receptors. Eur J Biochem 1994;225:827–843.
5. Shire D, Calandra B, Bouaboula M, et al. Cannabinoid receptor interactions with the antagonists SR 141716A and SR 144528. Life Sci 1999;65:627–635.
6. Shire D, Calandra B, Delpech M, et al. Structural features of the central cannabinoid CB1 receptor involved in the binding of the specific CB1 antagonist SR 141716A. J Biol Chem 1996;271:6941–6946.
7. Ramirez-Alvarado R, Serrano L, Blanco FJ. Conformational analysis of peptides corresponding to all the secondary structure elements of protein L B1 domain. Prot Sci 1997;6:162–174.
8. Song ZH, Slowey C-A, Hurst DP, Reggio PH. The difference between the CB1 and CB2 cannabinoid receptors at position 5.46 is crucial for the selectivity of WIN55212-2 for CB2. Mol Pharmacol 1999;56:834–840.
9. Gouldson P, Calandra B, Legoux P, et al. Mutational analysis and molecular modeling of the antagonist SR 144528 binding site on the human cannabinoid CB2 receptor. Eur J Pharmacol 2000;401: 17–25.
10. Tao Q, Abood ME. Mutation of a highly conserved aspartate residue in the second transmembrane domain of the cannabinoid receptors, CB1 and CB2, disrupts G-protein coupling. J Pharmacol Exp Ther 1998;285:651–658.
11. Bramblett RD, Panu AM, Ballesteros JA, Reggio PH. Construction of a 3D model of the cannabinoid CB1 receptor: determination of helix ends and helix orientation. Life Sci 1995;56:1971–1982.
12. Mahmoudian M. The cannabinoid receptor: computer-aided molecular modeling and docking of ligand. J Mol Graph Model 1997;15:149–53, 179.
13. Shire D, Calandra B, Gouldson P, et al. 1998 Symposium on the Cannabinoids; International Cannabinoid Research Society. Burlington, VT,; 1998:p.86.
14. Baldwin JM, Schertler GF, Unger VM. An alpha-carbon template for the transmembrane helices in the rhodopsin family of G-protein-coupled receptors. J Mol Biol 1997;272:144–164.
15. Kajihara A, Komooka H, Kamiya K, et al. Three-dimensional model of the human PAF receptor. J. Lipid Mediat Cell Signal 1994;9:185–196.
16. Hibert MF, Trumpp-Kallmeyer S, Bruinvels A, Hoflack J. Three-dimensional models of neurotransmitter G-binding protein-coupled receptors. Mol Pharmacol 1991;40:8–15.
17. Teeter MM, Froimowitz M, Stec B, DuRand CJ. Homology modeling of the dopamine D2 receptor and its testing by docking of agonists and tricyclic antagonists. J Med Chem 1994;37:2874–2888.
18. Henderson R, Baldwin JM, Ceska TA, Zemlin F, Beckmann E, Downing KH. Model for the structure of bacteriorhodopsin based on high-resolution electron cryo-microscopy. J Mol Biol 1990;213: 899–929.
19. Baldwin JM. The probable arrangement of the helices in G protein-coupled receptors. EMBO J 1993;12:1693–1703.
20. MSI-Biosym InsightII/Homology v98. MSI Inc, San Diego, CA.
21. Richardson JS. The anatomy and taxonomy of protein structure. Adv Protein Chem 1981;34:167–339.
22. Bockaert J, Pin JP. Molecular tinkering of G protein-coupled receptors: an evolutionary success. EMBO J 1999;18:1723–1729.
23. Chang YT, Loew GH. Construction and evaluation of a three-dimensional structure of cytochrome P450choP enzyme (CYP105C1). Protein Eng 1996;9:755–766.
24. Vriend G, Horn F. GPCRDB: Information system for G protein-coupled receptors (GPCRs). http://www.gpcr.org/; 2002.
25. Shire D, Calandra B, Rinaldi-Carmona M, et al. Molecular cloning, expression and function of the murine CB2 peripheral cannabinoid receptor. Biochim Biophys Acta 1996;1307:132–136.
26. Gebremedhin D, Lange AR, Aebly MR, Camphell WB, Hillard CJ, R. HD. Submitted (Mar-1997) to the EMBL/GenBank/DDBJ databases.
27. Matsuda LA, Lolait SJ, Brownstein MJ, Young AC, Bonner TI. Structures of a cannabinoid receptor and functional expression of the cloned cDNA. Nature (London) 1990;346:561–564.
28. Gerard C, Mollereau C, Vassart G, Parmentier M. Nucleotide sequence of a human cannabinoid receptor cDNA. Nucleic Acids Res 1990;18:7142.
29. Pritchett DB, Bach AW, Wozny M, et al. Structure and functional expression of cloned rat serotonin 5HT-2 receptor. EMBO J 1988;7:4135–4140.
30. Monsma FJ, Jr., Mahan LC, McVittie LD, Gerfen CR, Sibley DR. Molecular cloning and expression of a D1 dopamine receptor linked to adenylyl cyclase activation. Proc Natl Acad Sci USA 1990;87:6723–6727.
31. Lanier SM, Downing S, Duzic E, Homcy CJ. Isolation of rat genomic clones encoding subtypes of the alpha 2- adrenergic receptor. Identification of a unique receptor subtype. J Biol Chem 1991;266:10470–10478.
32. Lai J, Smith TL, Mei L, et al. The molecular properties of the M1 muscarinic receptor and its regulation of cytosolic calcium in a eukaryotic gene expression system. Adv Exp Med Biol 1991;287: 313–330.
33. Schuler GD, Altschul SF, Lipman DJ. A workbench for multiple alignment construction and analysis. Proteins 1991;9:180–190.
34. Dayhoff MO, Barker WC, Hunt LT. Establishing homologies in protein sequences. Methods Enzymol 1983;91:524–545.
35. Claverie JM, Daulmerie C. Smoothing profiles with sliding windows: better to wear a hat! Comput Appl Biosci 1991;7:113–115.
36. Kyte J, Doolittle RF. A simple method for displaying the hydropathic character of a protein. J Mol Biol 1982;157:105–132.
37. Ponder JW, Richards FM. Tertiary templates for proteins. Use of packing criteria in the enumeration of allowed sequences for different structural classes. J Mol Biol 1987;193:775–791.
38. Greenfield NJ, Montelione GT, Farid RS, Hitchcock-DeGregori SE. The structure of the N-terminus of striated muscle alpha-tropomyosin in a chimeric peptide: nuclear magnetic resonance

structure and circular dichroism studies. Biochemistry 1998;37: 7834–7843.
39. Choi G, Landin J, Xie XQ. The cytoplasmic helix of cannabinoid receptor CB2, a conformational study by circular dichroism and (1)H NMR spectroscopy in aqueous and membrane-like environments. J Pept Res 2002;60:169–177.
40. SYBYL. Molecular modeling software packages. version 6.8 ed: TRIPOS, associates, Inc, St Louis, MI63144; 2001.
41. Riek RP, Rigoutsos I, Novotny J, Graham RM. Non-alpha-helical elements modulate polytopic membrane protein architecture. J Mol Biol 2001;306:349–362.
42. Teller DC, Okada T, Behnke CA, Palczewski K, Stenkamp RE. Advances in determination of a high-resolution three-dimensional structure of rhodopsin, a model of G-protein-coupled receptors (GPCRs). Biochemistry 2001;40:7761–7772.
43. Jensen AD, Guarnieri F, Rasmussen SG, Asmar F, Ballesteros JA, Gether U. Agonist-induced conformational changes at the cytoplasmic side of transmembrane segment 6 in the beta 2 adrenergic receptor mapped by site-selective fluorescent labeling. J Biol Chem 2001;276:9279–9290.
44. Gerber BO, Meng EC, Dotsch V, Baranski TJ, Bourne HR. An activation switch in the ligand binding pocket of the C5a receptor. J Biol Chem 2001;276:3394–3400.
45. Tao Q, McAllister SD, Andreassi J, et al. Role of a conserved lysine residue in the peripheral cannabinoid receptor (CB2): evidence for subtype specificity. Mol Pharmacol 1999;55:605–613.
46. Song Z-H, Bonner TI. A lysine residue of the cannabinoid receptor is critical for receptor recognition by several agonists but not WIN55212-2. Mol Pharmacol 1996;49:891–896.
47. Ballesteros JA, Jensen AD, Liapakis G, et al. Activation of the beta 2-adrenergic receptor involves disruption of an ionic lock between the cytoplasmic ends of transmembrane segments 3 and 6. J Biol Chem 2001;276:29171–29177.
48. Visiers I, Ballesteros JA, Weinstein H. Three-dimensional representations of G protein-coupled receptor structures and mechanisms. Methods Enzymol 2002;343:329–371.
49. Shapiro DA, Kristiansen K, Weiner DM, Kroeze WK, Roth BL. Evidence for a model of agonist-induced activation of 5- hydroxytryptamine 2A serotonin receptors that involves the disruption of a strong ionic interaction between helices 3 and 6. J Biol Chem 2002;277:11441–11449.
50. Abood ME, Tao Q, Mcallister SD, Hurst DP, Norris J, Reggio PH. 1998 Symposium on the Cannabinoids, International Cannabinoid Research Society 2-2. Burlington, Vermont; 1998.
51. Feng W, Song ZH. Functional roles of the tyrosine within the NP(X)(n)Y motif and the cysteines in the C-terminal juxtamembrane region of the CB2 cannabinoid receptor. FEBS Lett 2001;501: 166–170.
52. Karnik SS, Khorana HG. Assembly of functional rhodopsin requires a disulfide bond between cysteine residues 110 and 187. J Biol Chem 1990;265:17520–17524.
53. Kurtenbach E, Curtis CA, Pedder EK, Aitken A, Harris AC, Hulme EC. Muscarinic acetylcholine receptors. Peptide sequencing identifies residues involved in antagonist binding and disulfide bond formation. J Biol Chem 1990;265:13702–13708.
54. Dohlman HG, Caron MG, DeBlasi A, Frielle T, Lefkowitz RJ. Role of extracellular disulfide-bonded cysteines in the ligand binding function of the beta 2-adrenergic receptor. Biochemistry 1990;29: 2335–2342.
55. Lu R, Hubbard JR, Martin BR, Kalimi MY. Roles of sulfhydryl and disulfide groups in the binding of CP-55,940 to rat brain cannabinoid receptor. Mol Cell Biochem 1993;121:119–126.
56. Higashijima T, Burnier J, Ross EM. Regulation of Gi and Go by mastoparan, related amphiphilic peptides, and hydrophobic amines. Mechanism and structural determinants of activity. J Biol Chem 1990;265:14176–14186.
57. Whiles JA, Brasseur R, Glover KJ, Melacini G, Komives EA, Vold RR. Orientation and effects of mastoparan X on phospholipid bicelles. Biophys J 2001;80:280–293.
58. Losonczi JA, Olejniczak ET, Betz SF, Harlan JE, Mack J, Fesik SW. NMR studies of the anti-apoptotic protein Bcl-xL in micelles. Biochemistry 2000;39:11024–11033.
59. Johnson JE, Cornell RB. Amphitropic proteins: regulation by reversible membrane interactions (review). Mol Membr Biol 1999; 16:217–235.
60. Mukhopadhyay S, McIntosh HH, Houston DB, Howlett AC. The CB(1) cannabinoid receptor juxtamembrane C-terminal peptide confers activation to specific G proteins in brain. Mol Pharmacol 2000;57:162–170.
61. Bechinger B, Kim Y, Chirlian LE, et al. Orientations of amphipathic helical peptides in membrane bilayers determined by solid-state NMR spectroscopy. J Biomol NMR 1991;1:167–173.
62. Schertler GFX, Villa C, Henderson R. Projection structure of rhodopsin. Nature (London) 1993;362:770–772.
63. Shirai H, Takahashi K, Katada T, Inagami T. Mapping of G protein coupling sites of the angiotensin II type 1 receptor. Hypertension 1995;25:726–730.
64. Wakamatsu K, Okada A, Miyazawa T, Ohya M, Higashijima T. Membrane-bound conformation of mastoparan-X, a G-protein-activating peptide. Biochemistry 1992;31:5654–5660.